Numerical Simulation of the Atmospheric Response to the Time-Varying El Niño SST Anomalies during May 1982 Through October 1983

M. J. FENNESSY AND J. SHUKLA

Center for Ocean–Land–Atmosphere Interactions, Department of Meteorology, University of Maryland, College Park, Maryland

(Manuscript received 15 June 1987, in final form 25 September 1987)

ABSTRACT

A general circulation model was first integrated for 25 months with monthly climatological boundary conditions of sea surface temperature (SST), soil moisture, sea ice and albedo. Starting from day 165 of this "control" integration, which corresponds to 1 May, another 18-month integration was carried out in which all the boundary conditions were the same as in the control run, except that the observed monthly SST anomalies for May 1982–October 1983 were added to the climatological values in the Pacific from 40°S to 60°N.

Monthly and seasonal means of the differences between the two integrations were compared to the observed atmospheric anomalies during the record El Niño warm SST event of 1982–83. The evolution of the strong atmospheric anomalies observed in the tropics was well simulated for the entire 18-month period. There were considerable differences in the extratropics between simulated and observed seasonal anomalies.

The highly successful anomaly simulation in the tropics is encouraging in light of the recent successes of tropical ocean modelers and suggests the possibility of obtaining useful long-term climate forecasts from a coupled ocean–atmosphere model.

1. Introduction

An important development in our understanding of the mechanisms for interannual variability of the global circulation has come with the recognition that changes in the boundary forcings at the earth's surface [sea surface temperature (SST), soil moisture, snow cover, sea ice, etc.] are strongly related to changes in the atmospheric circulation (Shukla, 1984). The time scales of air–sea–land interactions can be much larger than the limit of deterministic predictability, and therefore a successful modeling of these interactions gives hope for dynamical extended-range prediction. An outstanding example of long-period air–sea interaction is the El Niño–Southern Oscillation phenomena which has been a subject of extensive observational and modeling studies during recent years (Rasmusson and Wallace, 1983). A large body of observational evidence documenting the relationship between SST anomalies in the Pacific Ocean and global atmospheric circulation has already appeared in the meteorological literature. The existence of highly significant empirical relationships between SST anomalies and atmospheric circulation anomalies has also encouraged the modeling community to carry out controlled numerical experiments with global general circulation models (GCMs). The success of such modeling studies in simulating the essential features of observed large-scale atmospheric circulation anomalies and similar successes of tropical ocean models in simulating the SST anomalies using observed atmospheric forcing has become a source of considerable optimism for extended-range prediction of the coupled atmosphere–ocean system.

The present study is an attempt to simulate the atmospheric circulation anomalies corresponding to the observed SST anomalies in the Pacific Ocean for the 18-month period May 1982–October 1983. Before we describe the actual results of this study, we briefly review the earlier modeling studies to investigate model sensitivity to Pacific SST anomalies.

Most, if not all, of the earlier GCM sensitivity studies can be classified into the following broad categories: (a) equilibrium response to a fixed SST anomaly; (b) short-term transient response for periods ranging from one month to one season, to a fixed or slowly varying SST anomaly, for a particular initial state; (c) long-term transient response to a time-varying SST anomaly for periods beyond a season.

It may be fair to say that some of the reasons that various modeling groups conducted these different types of sensitivity studies had more to do with the kind of model and computing facilities that were available to them rather than following a predetermined experimental design. Nonetheless, in retrospect it is not unreasonable to classify them in this framework and draw some general conclusions:

- *Equilibrium response:* These are classical sensitivity experiments in which a GCM is integrated for a

Corresponding author address: Mr. Michael J. Fennessy, Center for Ocean–Land–Atmosphere Interactions, Department of Meteorology, University of Maryland, College Park, Maryland 20742.

sufficiently long time to obtain two equilibrium climates, one with and the other without the prescribed SST anomaly. The difference between the two mean climates is considered to be the effect of the prescribed SST anomaly. These integrations have been made using models with a seasonal cycle (Palmer and Mansfield, 1986a,b and without a seasonal cycle (Geisler et al., 1985). Results of such sensitivity studies do not necessarily give any clear indication of the short-term response. The calculated response, especially outside the tropics, strongly depends upon the mean climate of the model.

- *Short-term transient response:* The main motivation for these experiments is to investigate the manner in which the imposition of a SST anomaly produces changes in circulation and rainfall during the first 30–90 days (Fennessy et al., 1985; Tokioka et al., 1985; and papers in WMO, 1986). These experiments help determine the possible impact of observed SST anomalies on dynamical prediction of monthly and seasonal averages and have suggested that the midlatitude response strongly depends upon the structure of the initial condition of the atmosphere.
- *Long-term transient response:* Experiments of this type attempt to investigate the role of SST anomalies in producing interannual variability of atmospheric circulation and rainfall. These experiments can also be useful to study the predictability of the coupled ocean–atmosphere system, because prescription of the observed SST anomalies can be considered to be equivalent to having a perfect ocean model. A recent paper by Lau (1985), in which he investigated the interannual variability of the model-simulated atmospheric circulation with observed SST anomalies prescribed over the tropical Pacific during the period 1962–76, falls into this category.

The present study also falls in this category, although it differs from Lau's study in many important respects. In Lau's work, the primary emphasis was put on the investigation of the mean composite response due to all the warm events averaged together, and on statistical relationships (correlation coefficients) between SST anomalies and circulation anomalies. In the present paper we have used the observed SST anomalies only for the 1982–83 warm episode, and we compare the evolution of the model-simulated circulation and rainfall anomalies to the actual observations for the same period.

Compared to earlier events, the 1982–83 El Niño warm tropical Pacific sea surface temperature event was of unusually large magnitude and extent. At its peak, during the Northern Hemisphere (NH) winter, the warm SST anomaly covered most of the tropical Pacific and reached magnitudes of over 4°C locally. Concurrent atmospheric anomalies were extraordinary in both the tropics and the extratropics (Quiroz, 1983). In the tropics, strong low-level wind and precipitation anomalies developed in the central equatorial Pacific in June 1982 and expanded eastward while intensifying in the following months. Meanwhile, droughts developed over Indonesia, Australia and northeast Brazil, while along portions of the western coast of South America, record rainfall was reported. Among the large anomalies in the extratropics was a record negative 700 mb geopotential height anomaly in the vicinity of the Aleutians.

Several researchers (see papers in Nihoul, 1985) studied the response of general circulation models to the 1982/83 El Niño mature phase December, January, and February (DJF) SST anomalies. In general, they found that the DJF SST anomalies were capable of causing anomalies in the simulated tropical pressure, wind and precipitation fields similar to those observed during the mature phase of the 1982/83 event. These studies did not address the evolution of the atmospheric anomalies, which was particularly striking in the tropics, with an eastward progression of strong wind and precipitation anomalies from June 1982 through July 1983.

In the current study we show that the time evolution of the simulated monthly mean circulation and rainfall anomalies in the tropics is remarkably similar to the observations for the same 18-month period.

2. The model, integrations and boundary conditions

Two integrations were performed with the Goddard Laboratory for Atmospheric Sciences (GLAS) climate model used and described by Fennessy et al. (1985). The model is global in extent with nine sigma levels in the vertical and a 4° lat by 5° long grid. The Matsuno scheme is used for time integration with a 7½ min time step. Convective clouds are limited to the lowest six levels and do not interact with radiation. Supersaturation clouds occur at all nine levels, but only the lowest six levels interact with radiation. The planetary boundary layer (PBL) is that of Deardorff (1972) as modified by Randall (1976).

The 25-month control integration was started from observed initial conditions for 0000 UTC on 15 November 1978 obtained from the National Meteorological Center (NMC). Annually varying climatological monthly mean values of SST, sea ice and surface albedo were interpolated to daily values for use in the control integration. These climatological boundary conditions are the same as those used and described by Fennessy et al. (1985).

The second integration of 18-months length, which we will refer to as the boundary integration, was started from day 165 of the control integration, corresponding to 1 May. This integration differed from the control integration only in that the observed monthly mean SST anomalies over the Pacific Ocean from 40°S to 60°N for May 1982–October 1983, obtained from the Climate Analysis Center (CAC), were added to the monthly climatological SST field used in the control integration. The resulting 18 monthly SST fields, re-

sembling the observed monthly SST fields in this region of the Pacific for May 1982–October 1983, were interpolated to daily values for model integration.

During the summer of 1982 there was a large region of SST anomalies greater than 1°C across the eastern and central tropical Pacific (Fig. 1a). This anomaly expanded and intensified throughout the fall so that by the winter of 1982–83 the 1°C anomaly extended

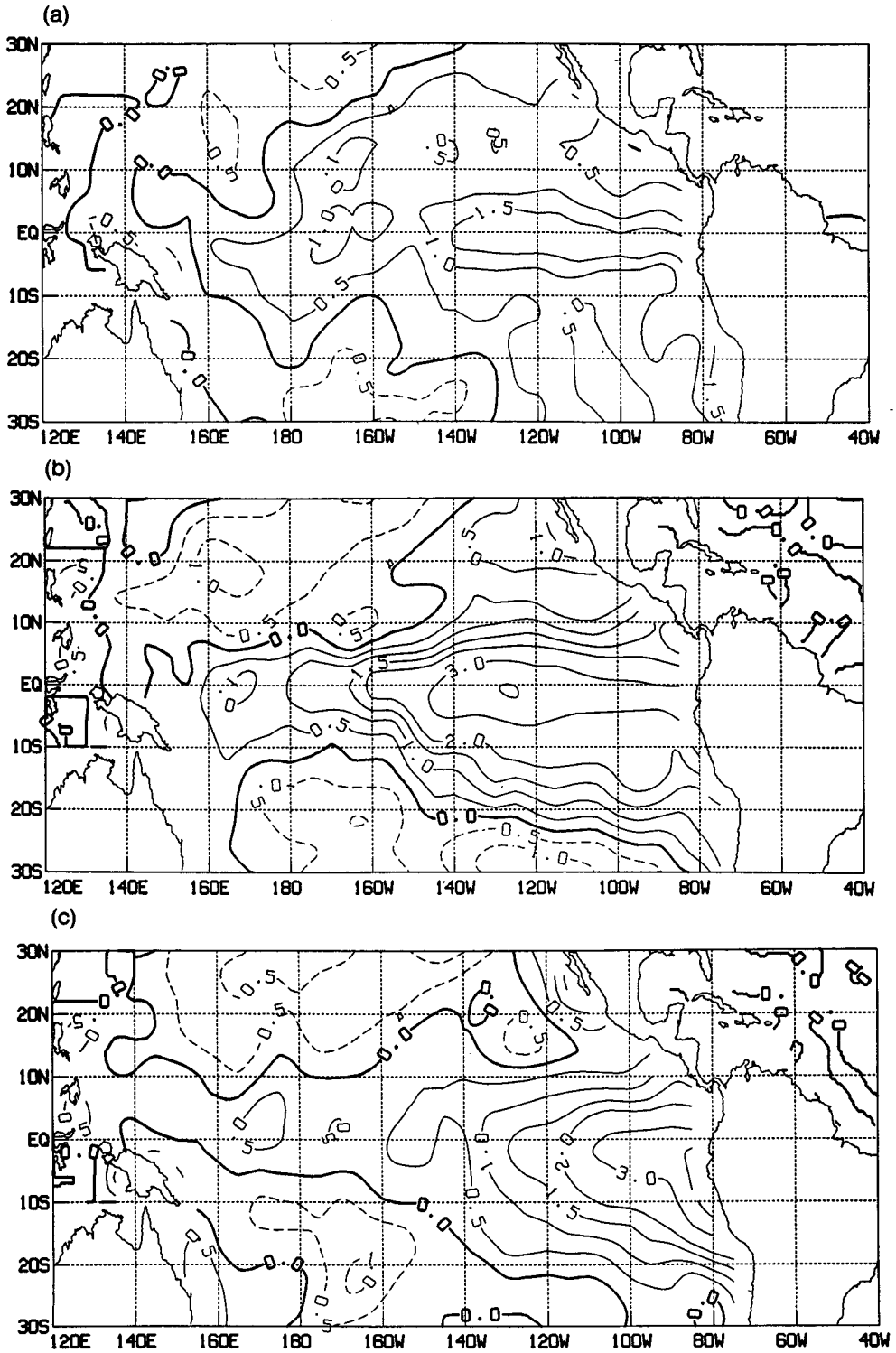

FIG. 1. Seasonal mean sea surface temperature anomaly for (a) JJA 1982, (b) DJF 1982/83, and (c) JJA 1983. Contours are 0, ±0.5, 1, 1.5, 2, 3 and 4°C. Dashed contours are negative.

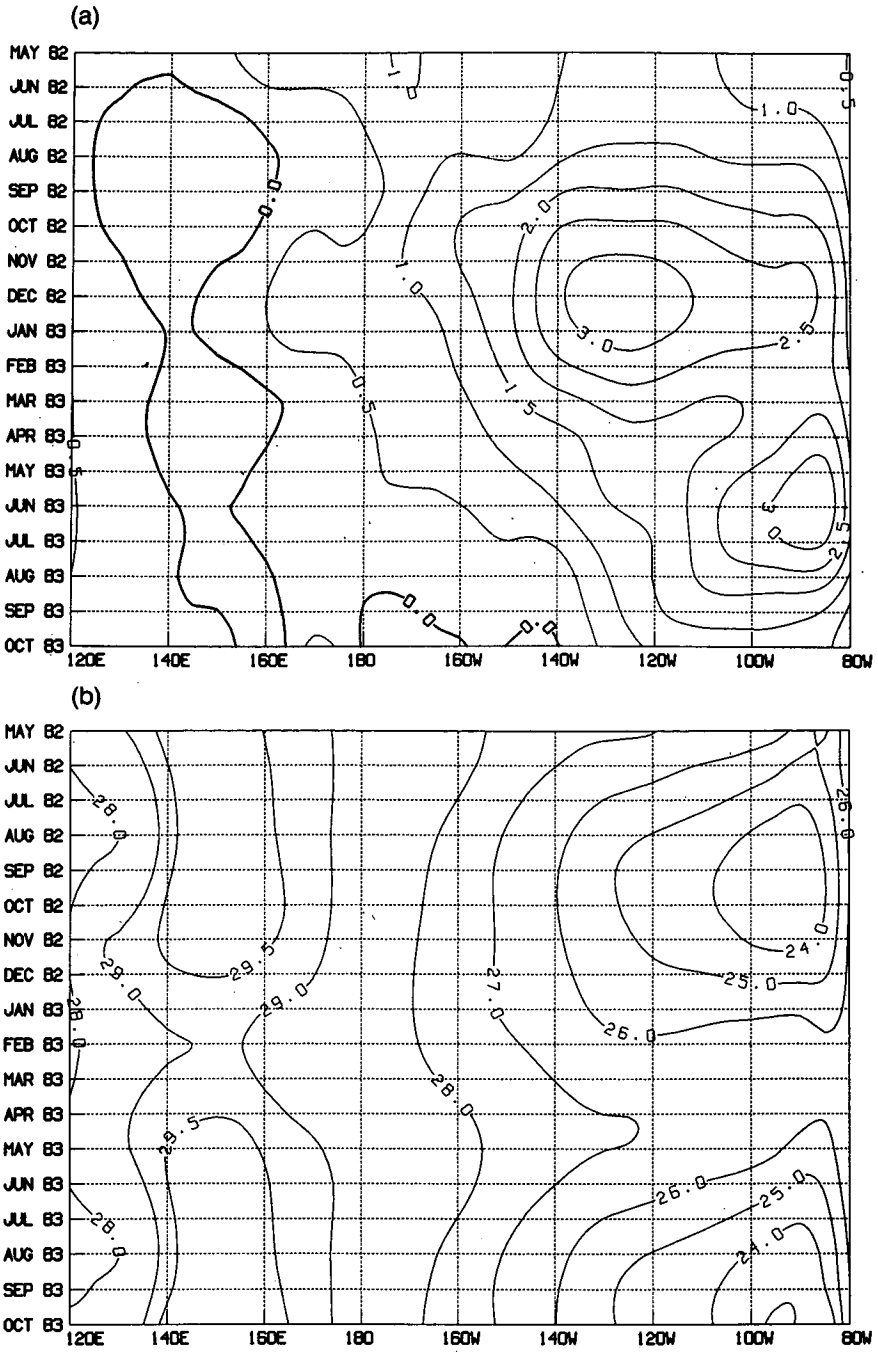

FIG. 2. Longitude–time cross section of monthly 6°S–6°N sea surface temperature for (a) observed anomaly (contour interval is 0.5°C), (b) climatology used in control integration, and (c) 1982–83 used in boundary integration. (Contours for (b) and (c) are 23, 24, 25, 26, 27, 28, 29, 29.5, and 30°C). Starred line taken from Fig. 3a.

westward to 160°E and a 3°C anomaly was observed from the South American coast to 150°W along the equator (Fig. 1b). The maximum anomaly at this time exceeded 4°C in the vicinity of 125°W. The anomaly then contracted toward the east while intensifying along the South American coast. By the summer of 1983 the 1°C anomaly was confined to the east of 140°W, the 3°C anomaly was confined to the east of 110°W and the maximum anomaly of greater than 4°C was right along the South American coast (Fig. 1c). The time evolution of this unprecedented anomaly can be better viewed in a longitude–time cross section averaged from 6°S to 6°N (Fig. 2a) which clearly shows the eastward progression of the maximum SST anomaly.

It was noted by Shukla and Wallace (1983) for earlier GCM experiments and by Quiroz (1983) for obser-

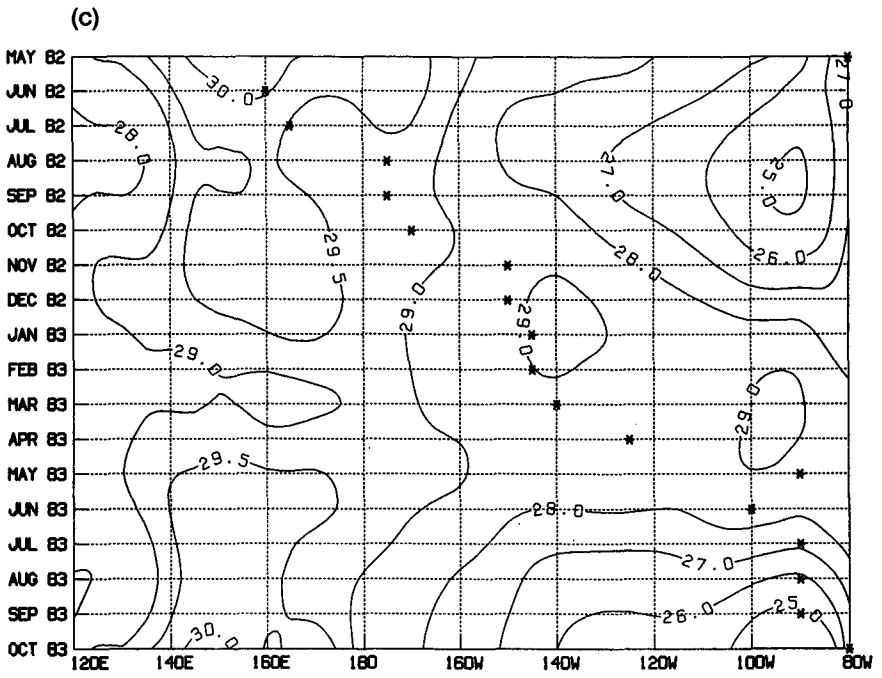

FIG. 2. (*Continued*)

vations that rainfall anomalies have a stronger association with the total SST field rather than with the SST anomalies themselves. The SST field used in the model control simulation is shown as a longitude–time cross section averaged from 6°S to 6°N in Fig. 2b, while that used in the boundary simulation is shown in Fig. 2c. It should be noted that climatologically, very warm (~29°C) water is restricted to the west of the dateline (control simulation), while during 1982–83 the warmest spot propagates eastward across the tropical Pacific (boundary simulation). The starred line in Fig. 2c is the axis of the maxima in the observed precipitation anomaly and will be discussed in section 3.

3. Results

Figures 3a and b show the observed and simulated rainfall anomalies, respectively. The observed precipitation anomalies were obtained by dividing the observed OLR anomalies in W m^{-2} by −5.7 (Arkin, personal communication). This is an empirical approximation based on 7 years of data over a small region in the equatorial Pacific, and thus must be used with caution. The observed maximum precipitation (minimum OLR) anomaly axis is drawn as a starred line on Fig. 3a as well as on Fig. 3b, which shows the boundary simulation minus control simulation precipitation difference. Hereafter, such differences will be referred to as simulated anomalies. A good correspondence between the observed and simulated precipitation anomalies is clearly demonstrated by comparing Fig. 3a to 3b. The simulated anomalies did, however, develop a little faster and farther to the east than those observed in the first couple of months. Otherwise, the time evolution and eastward propagation of both the positive and negative anomalies, even in their magnitudes, is well simulated. The maximum observed precipitation anomaly axis was also drawn on Fig. 2c to emphasize the close proximity of the maximum precipitation anomaly to the warmest mean SST.

The spatial pattern of the observed and simulated precipitation anomalies during DJF 1982/83 is shown in Figs. 4a and 4b, respectively. The magnitude and extent of the large positive anomaly in the central and eastern equatorial Pacific, as well as the negative anomalies to the west and flanking north and south are correctly simulated, although the negative anomaly to the west is somewhat different than the observed. The major deficiency is the poor simulation of the positive anomaly to the southeast, which represents the observed eastward shift in the South Pacific convergence zone (SPCZ). The SPCZ is poorly simulated in the control integration—a weakness of the model. Well simulated is the negative–positive anomaly dipole over eastern Brazil. The spatial scale of the simulated negative anomaly over Australia is so different compared to that observed that this anomaly could be merely fortuitous. It should be noted, however, that Australia and eastern Brazil both experienced important droughts during this period.

A 6°S–6°N longitude–time cross section of the observed precipitation during 1982–83 is shown in Fig. 5a. This is an approximate observed field obtained from the OLR using the following empirical relation based on 7 yr of data over a small region of the equatorial Pacific: precipitation (mm day^{-1}) = (25.4/30) × [63.9

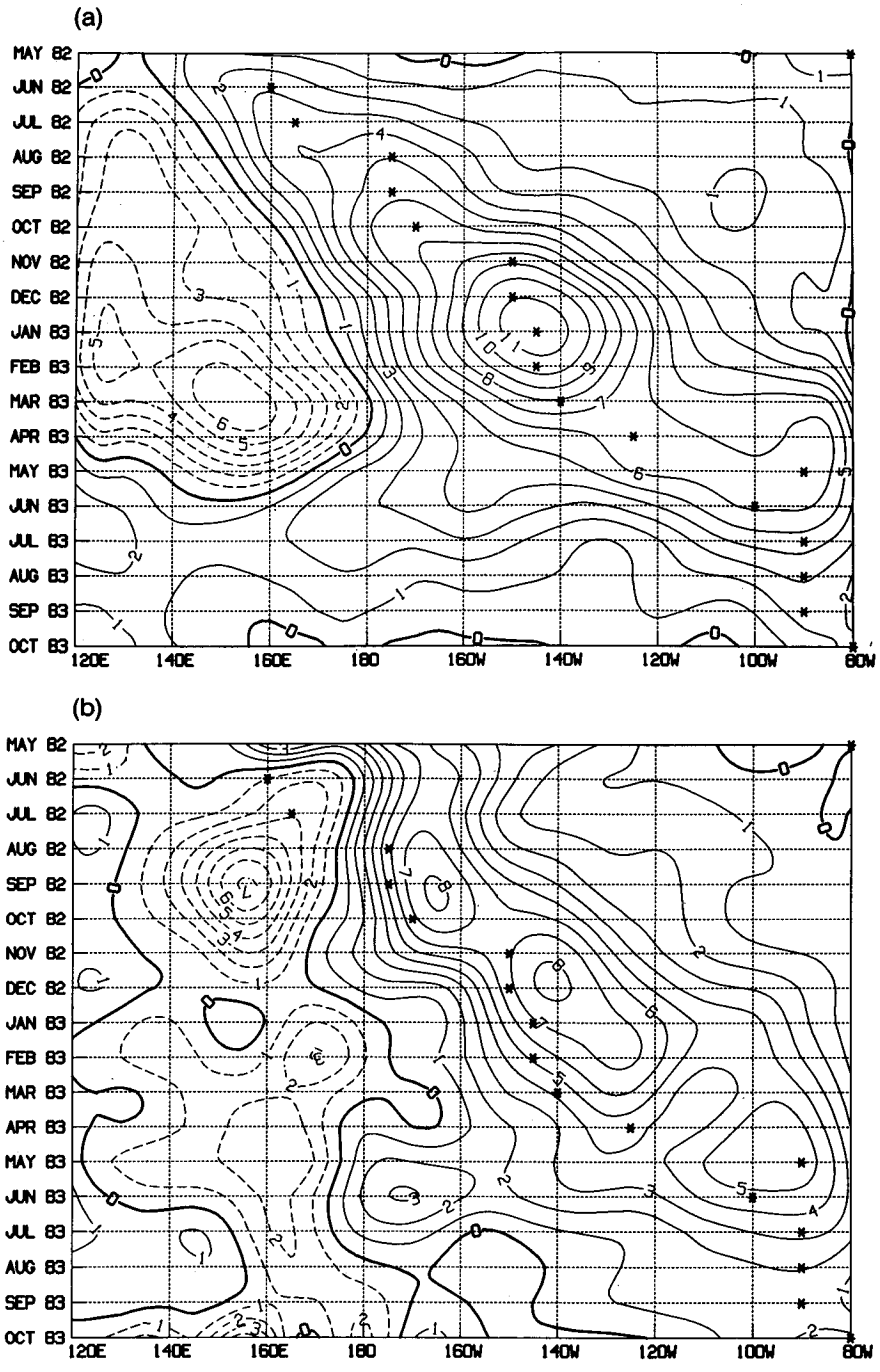

FIG. 3. Longitude–time cross section of monthly 6°S–6°N precipitation for (a) observed anomaly calculated from observed OLR anomaly, and (b) simulated anomaly. Contour interval is 1 mm day^{-1}. Dashed contours are negative. Starred line denotes axis of maximum observed precipitation anomaly.

$-0.22 \times$ OLR (W m^{-2})] (Arkin, personal communication). The same cross section of total precipitation in the boundary simulation (Fig. 5b) contains the observed eastward-shifting heavy precipitation across the central and eastern Pacific; however, the precipitation to the west remains too intense compared to that observed, and the precipitation in the east is a little weak during the later months of the simulation. These defects are inherent in the model control run simulation of precipitation which can be seen by comparing the ob-

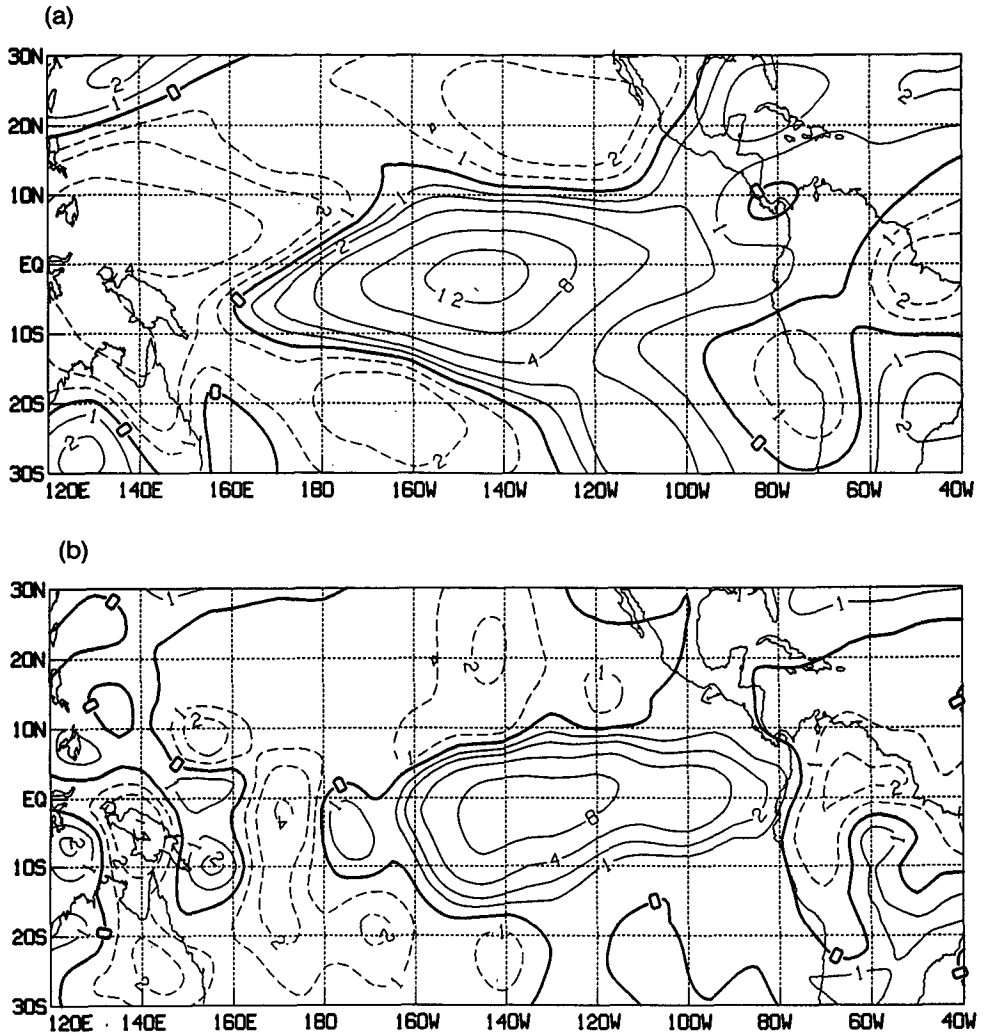

FIG. 4. The DJF 1982/83 mean precipitation for (a) observed anomaly calculated from observed OLR anomaly, and (b) simulated anomaly. Contours are 0, ±1, 2, 4, 8, and 12 mm day^{-1}. Dashed contours are negative.

served climatological precipitation field (Fig. 5c) with the model control simulation (Fig. 5d). This observed climatological precipitation field was obtained from 7 yr of OLR data using the empirical relation described above. The model-simulated heavy precipitation tends to persist throughout the year in the west Pacific near Indonesia.

It is interesting to compare the simulated precipitation anomalies during the NH winter of 1982/83 with those obtained in an earlier study (Fennessy et al., 1985), which used the same 1982/83 SST anomalies in a shorter simulation with the same model. Figure 6a shows the 11–60 day simulated precipitation anomalies from the Fennessy et al. simulations which started from observed initial conditions on 16 December 1982. The simulated anomalies for the same calendar period of the current integrations which were started more than 7 months earlier on 1 May are shown in Fig. 6b. The great similarity of the two maps is indicative of the dominance of boundary condition forcing on precipitation anomalies in the tropics. The differences in the western Pacific are reflective of the highly variable model precipitation in that region. Similar differences in the western Pacific precipitation are found among different model control simulations with identical boundary conditions.

Figure 7a shows the simulated anomaly of vertically integrated moisture flux convergence for DJF 1982/83. The remarkable similarity between this field and precipitation anomaly for the same period (Fig. 4b) suggests that most of the moisture required by the simulated precipitation anomalies was provided by moisture convergence anomalies. Only about 25% of the positive precipitation anomaly along the equator can

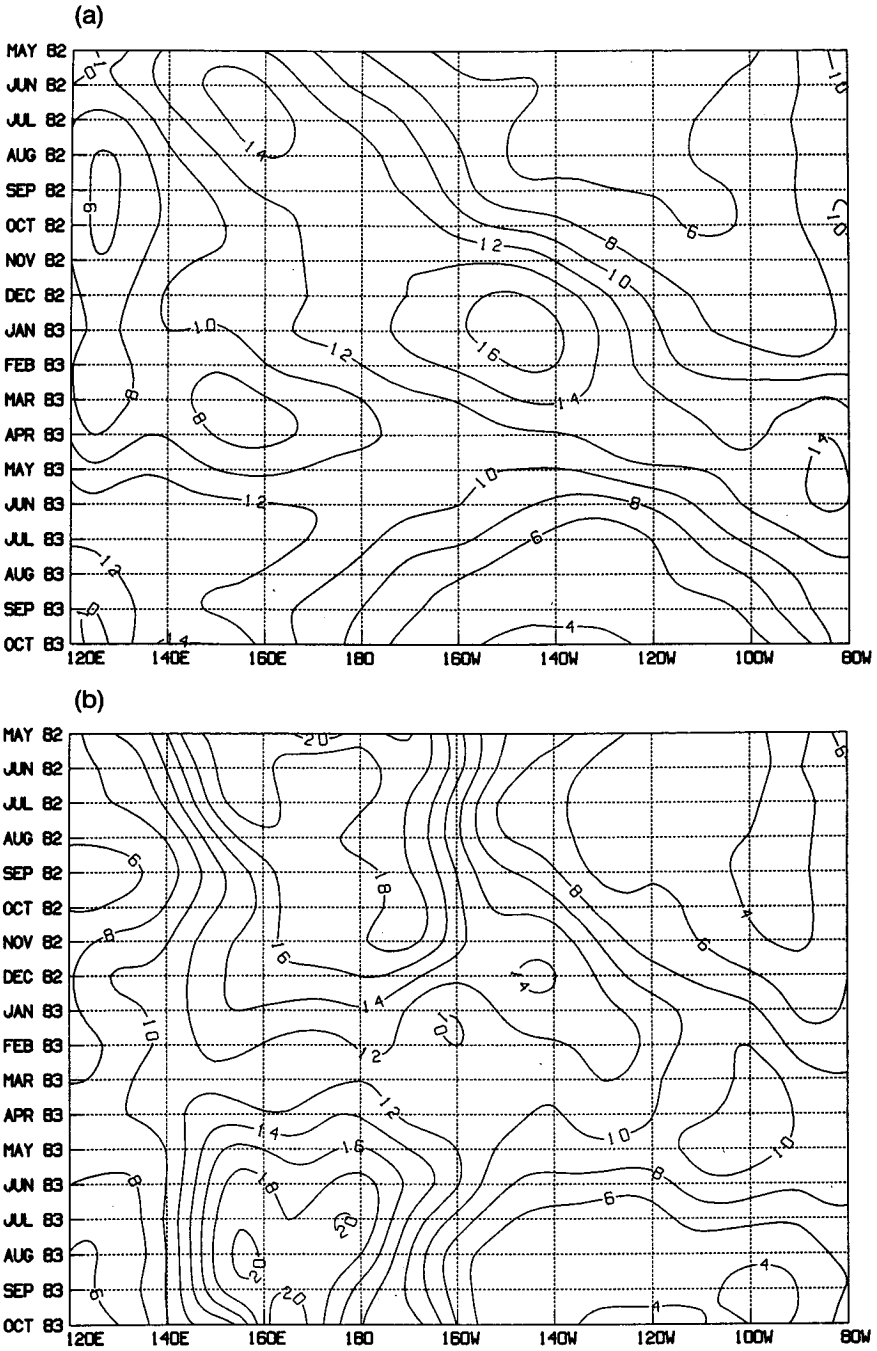

FIG. 5. Longitude–time cross section of 6°S–6°N precipitation for (a) 1982–83 observed monthly means calculated from observed OLR, (b) boundary integration monthly means, (c) observed monthly climatology calculated from 7 yr OLR climatology, and (d) control integration monthly means. Contour interval is 2 mm day^{-1}.

be accounted for by the evaporation anomaly (Fig. 7b), which reached a maximum of 3 mm day^{-1}. The negative precipitation anomalies to the north, south and west of the positive precipitation anomaly are entirely accounted for by negative moisture convergence anomalies. This also holds true for the precipitation deficits over Australia and NE Brazil. Simulated surface sensible heat flux anomalies (not shown) were small, contributing only about one-quarter as much to the surface energy balance anomalies, as did the evaporation anomalies.

The simulated sea level pressure anomaly field con-

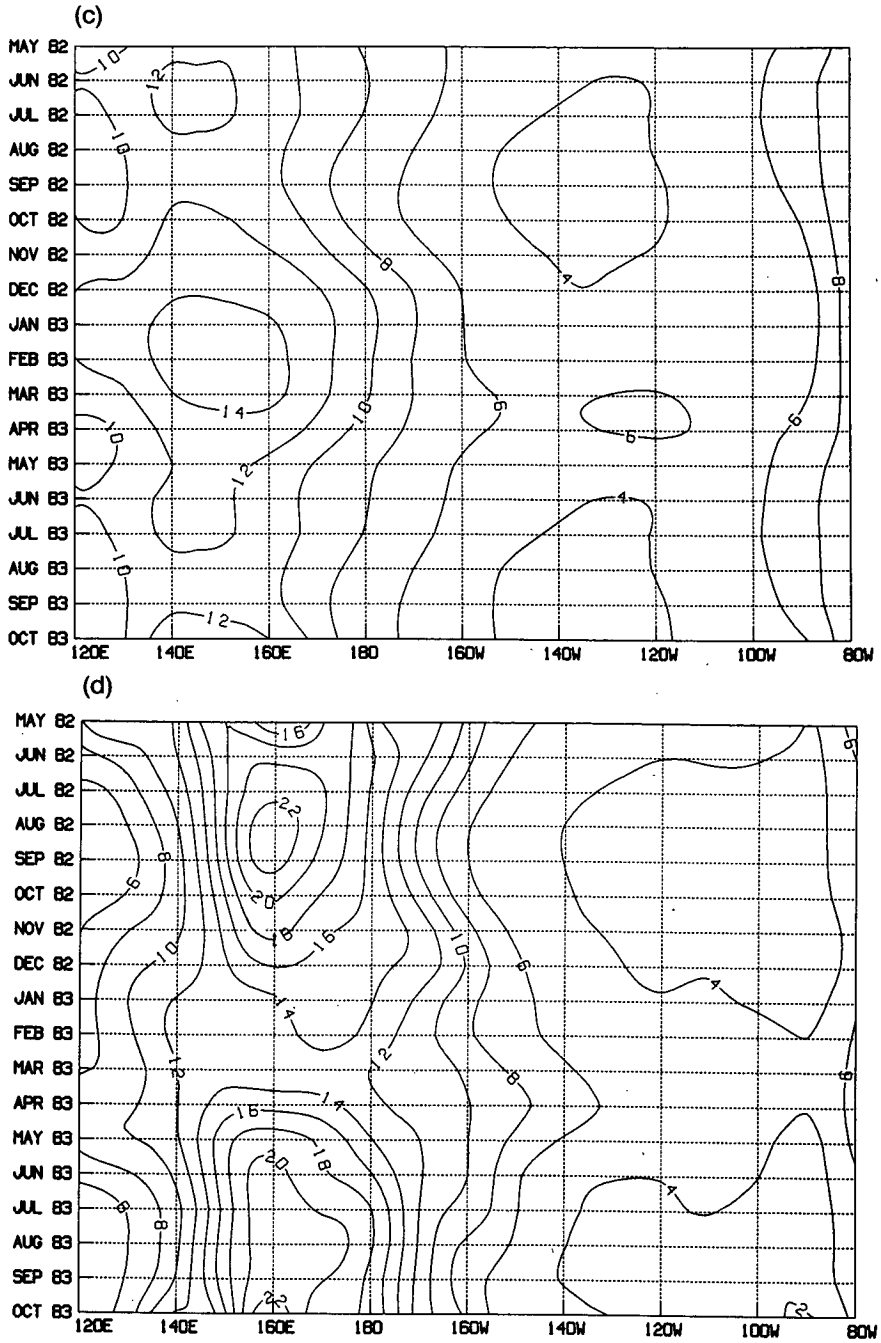

FIG. 5. (*Continued*)

tained a strong, negative Southern Oscillation signal as seen in a time–longitude cross section averaged from 10°S–10°N (Fig. 8). This signal reached maximum amplitude in January and February 1983, coinciding with the timing of the observed minimum in the Southern Oscillation index (Quiroz, 1983).

The simulated low-level wind anomalies in the equatorial Pacific greatly resembled their observed counterparts. The eastward propagation of the observed westerly 850 mb wind anomalies can be seen in Fig. 9a, which was adapted from Arkin et al. (1983). A longitude–time cross section of the simulated 850 mb westerly wind anomalies (Fig. 9b) is very similar to that of the observed anomalies. The simulated westerly anomalies did, however, persist longer than those observed in the east Pacific during the latter months of the simulation.

Strong relative warming of the entire tropical at-

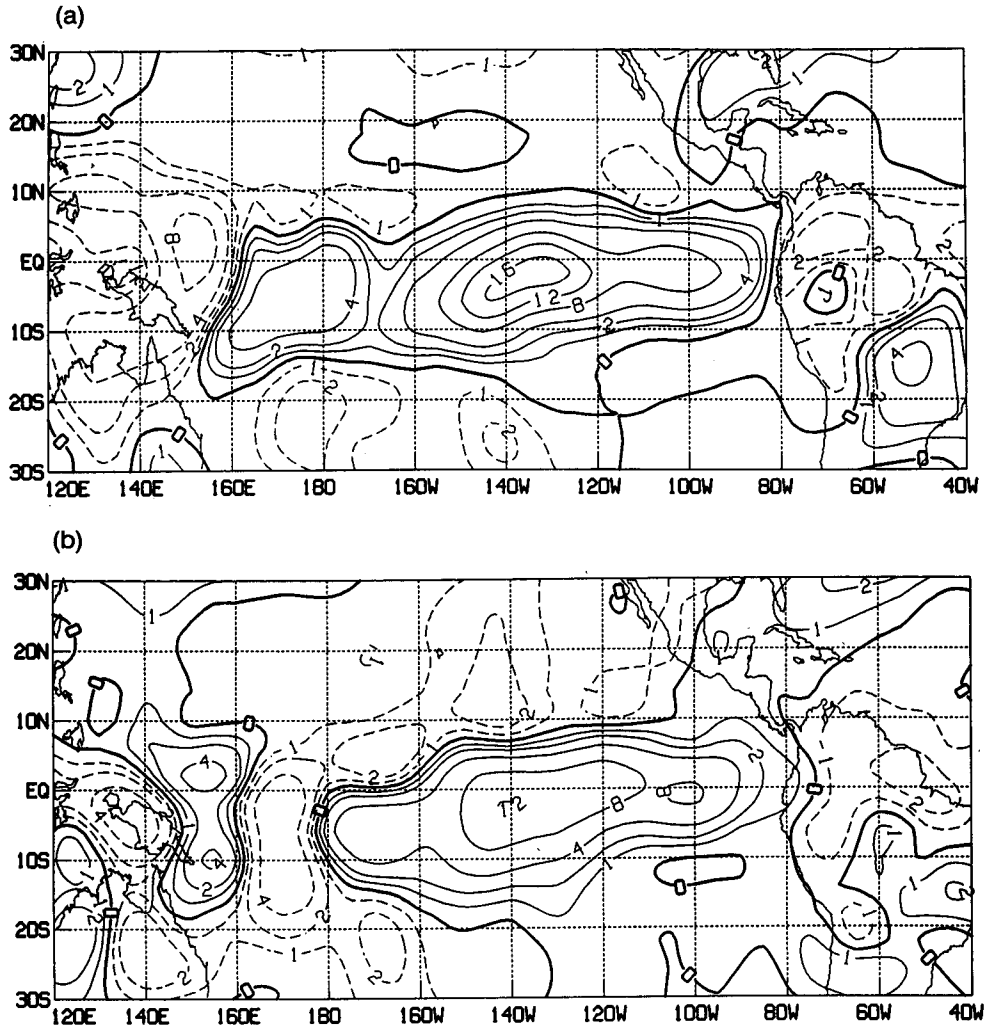

FIG. 6. Simulated precipitation anomalies for (a) 11–60 day average from Fennessy et al. (1985), 16 December 1982 initial condition case, and (b) 50 day average for same calendar period of current integrations. Contours are 0, ±1, 2, 4, 8, 12 and 16 mm day^{-1}. Dashed contours are negative.

mosphere occurred in the boundary simulation. There was a 60 m or more increase in the 200–1000 mb thickness averaged zonally from 30°S to 30°N (Fig. 10) from December 1982 through May 1983. This corresponds to a warming of the tropical troposphere of approximately 1.5°C or more, in reasonable agreement with observed temperature anomalies.

The model response at upper levels in the tropical Pacific was also quite realistic. Longitude–time cross sections of the observed 200 mb equatorial zonal wind anomalies (Fig. 11a, adapted from Arkin et al., 1983) and the simulated 200 mb zonal wind anomalies (Fig. 11b) both show strong easterly anomalies propagating eastward across the tropical Pacific. The maximum simulated negative anomaly reached 13 m s^{-1}, while the observed exceeded 20 m s^{-1}. This undersimulation of the anomaly is consistent with the magnitude of the local geopotential height response. The simulated easterly anomalies persisted through August 1983, 2 months longer than the observed easterly anomalies.

The simulated 300 mb geopotential height anomaly field contained anticyclonic couplets straddling the equator and shifting eastward while intensifying from the NH autumn of 1982 (Fig. 12a) to the NH winter of 1982/83 (Fig. 12b), although their magnitude was weaker than that observed. Both the NH autumn of 1982 and the spring of 1983 (Fig. 12c) simulated 300 mb geopotential height anomaly fields contained patterns over North America reminiscent of the observed anomaly pattern for the winter of 1982/83, particularly the strong negative anomaly in the vicinity of the Aleutians. However, the simulated geopotential height anomaly field for the winter of 1982/83 did not contain this pattern. We do not know whether the similarity between the observed DJF patterns and model-simulated NH fall 1982 and spring 1983 patterns is merely

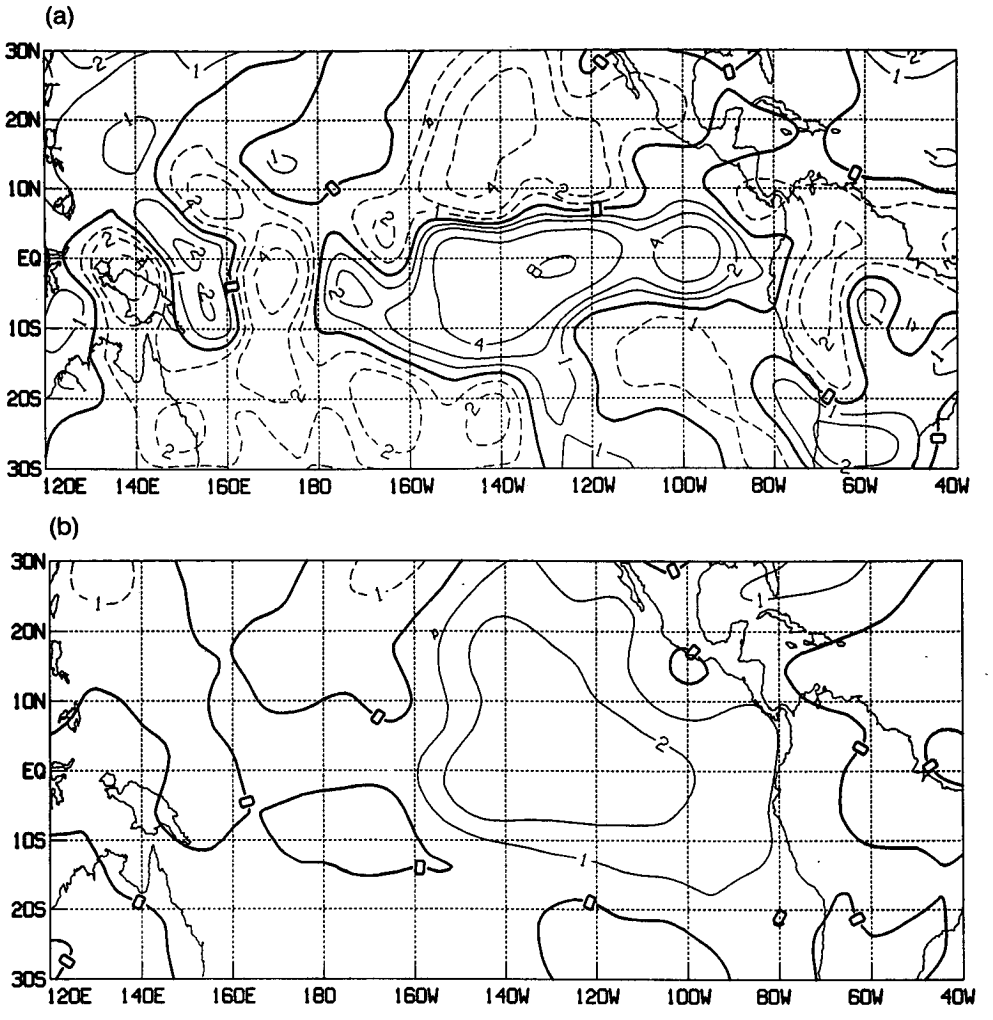

FIG. 7. The DJF 1982/83 simulated anomalies of (a) vertically integrated moisture convergence, and (b) surface evaporation. Contours are 0, ±1, 2, 4 and 8 mm day^{-1}. Dashed contours are negative.

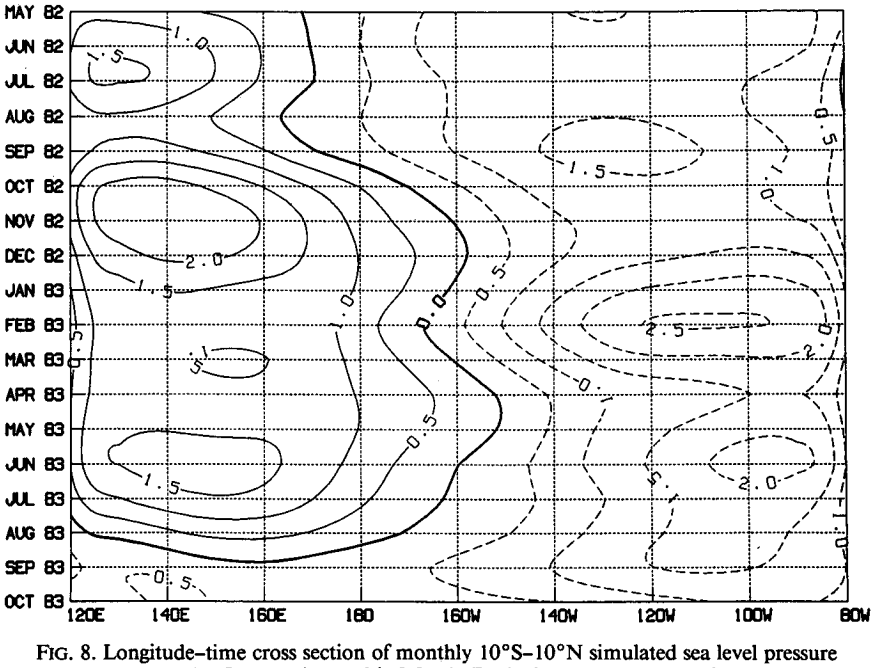

FIG. 8. Longitude–time cross section of monthly 10°S–10°N simulated sea level pressure anomaly. Contour interval is 0.5 mb. Dashed contours are negative.

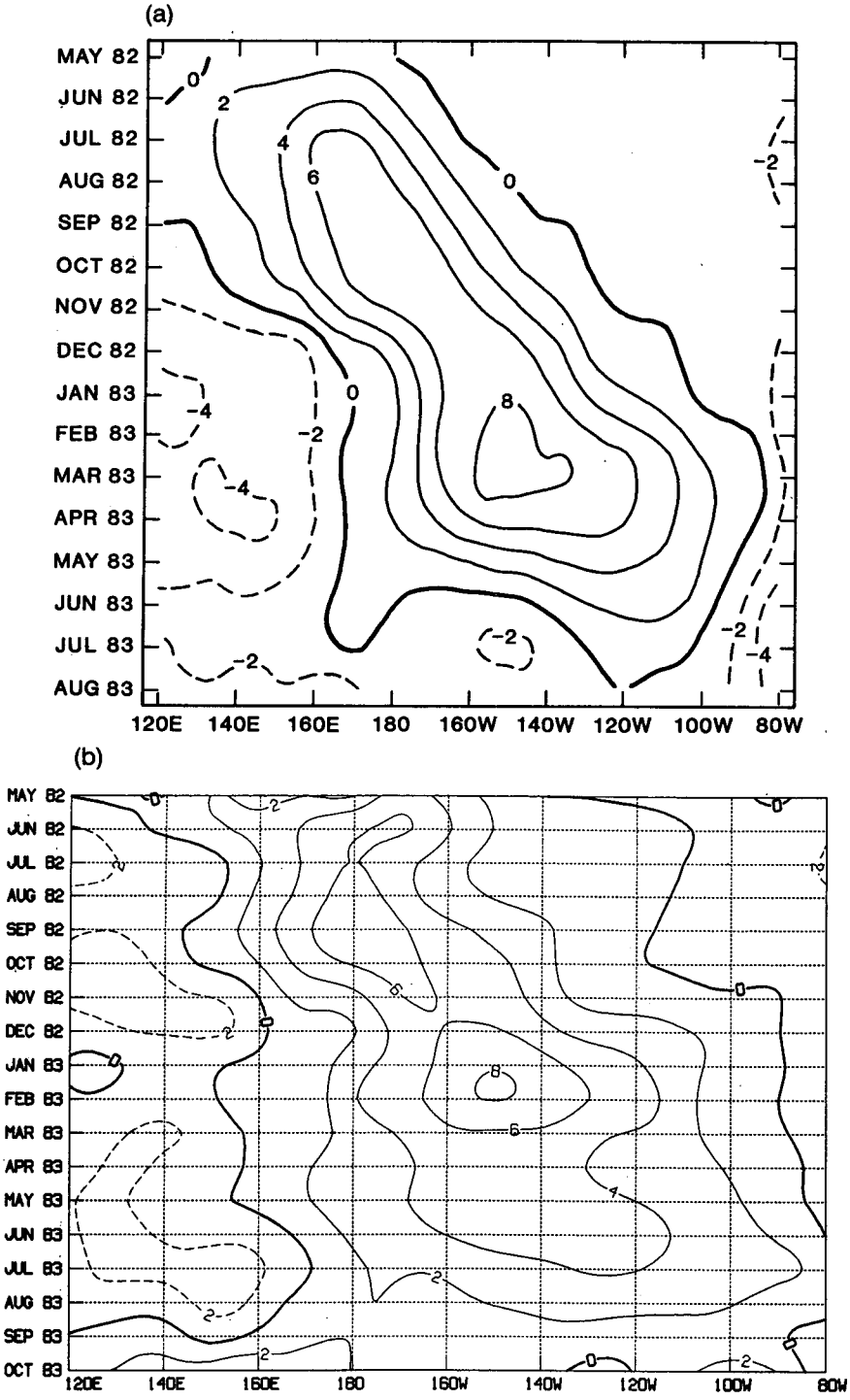

FIG. 9. Longitude–time cross section of monthly 850 mb zonal wind for (a) 1982–83 observed anomaly adopted from Arkin et al. (1983), and (b) simulated anomaly. Contour interval is 2 m s^{-1}. Dashed contours are negative.

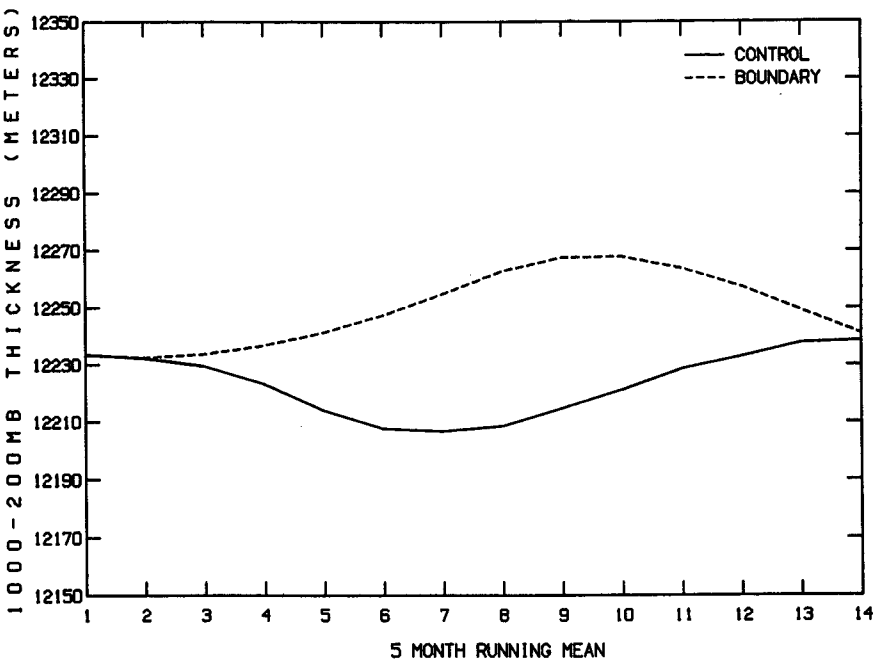

FIG. 10. Five-month running mean time series of zonally averaged 30°S–30°N, 200–1000 mb thickness (meters). Control integration is solid. Boundary integration is dashed.

due to chance. Considering the dependence of extratropical response on the mean climate of the model (Palmer and Mansfield, 1986a,b) and the large climate drift of the present model (Shukla and Fennessy, 1987), we do not expect to find great similarities between the model and the observed extratropical anomalies after more than 6 months of integration. We cannot, however, fail to note that averaged over the entire 18 months of the two simulations, the 300 mb westerly wind anomaly field (Fig. 13) clearly shows the 1982–83 ENSO signature of easterly anomalies over the tropical Pacific, intensified subtropical jets and easterly anomalies in midlatitudes.

4. Summary and conclusions

The GLAS atmospheric GCM was integrated twice over the 18-month period from 1 May to 1 November. The first, or control integration, was done using monthly climatological SST everywhere. The second, or boundary integration, used the same monthly climatological SST, except in the Pacific Ocean, where the CAC observed monthly SST anomalies for May 1982–October 1983 were added to the monthly climatology. The difference between the two integrations was compared to the observed atmospheric anomalies for May 1982–October 1983.

In the tropics, the striking evolution of the observed large positive precipitation anomaly and low-level wind anomalies propagating eastward throughout the period was very well simulated. The observed upper-level wind and height anomalies, as well as the strong negative Southern Oscillation SLP signal were also well simulated. The entire simulated tropical troposphere was warmed by the anomalous SST, as observed. These results reflect the dominance of surface boundary forcing in the tropics, particularly that of the Pacific SST. The importance of the total SST field, rather than just the SST anomalies, is witnessed by the close correspondence between the evolution of the total SST field and that of the OLR/precipitation anomalies. Large positive precipitation anomalies occur where the positive SST anomalies result in a very warm (~29°C) total SST. Overall, the excellent simulation of the evolution of the atmospheric anomalies in the tropics is encouraging for the problem of making extended-range forecasts with a coupled ocean–atmosphere model.

In the extratropics, the simulated anomalies were often not in phase temporally with similar observed anomalies. Recent research has shown the great importance of the mean flow in obtaining a realistic midlatitude response to tropical forcing. In long integrations, such as those presented here, the simulated mean flow has evolved quite differently from that observed. Thus, problems in the extratropical response are not surprising. Nevertheless, the fact that the ENSO signal remains in longer (approximately annual) time means is encouraging.

Finally, we should point out that these results are based on a single realization, and thus we cannot judge

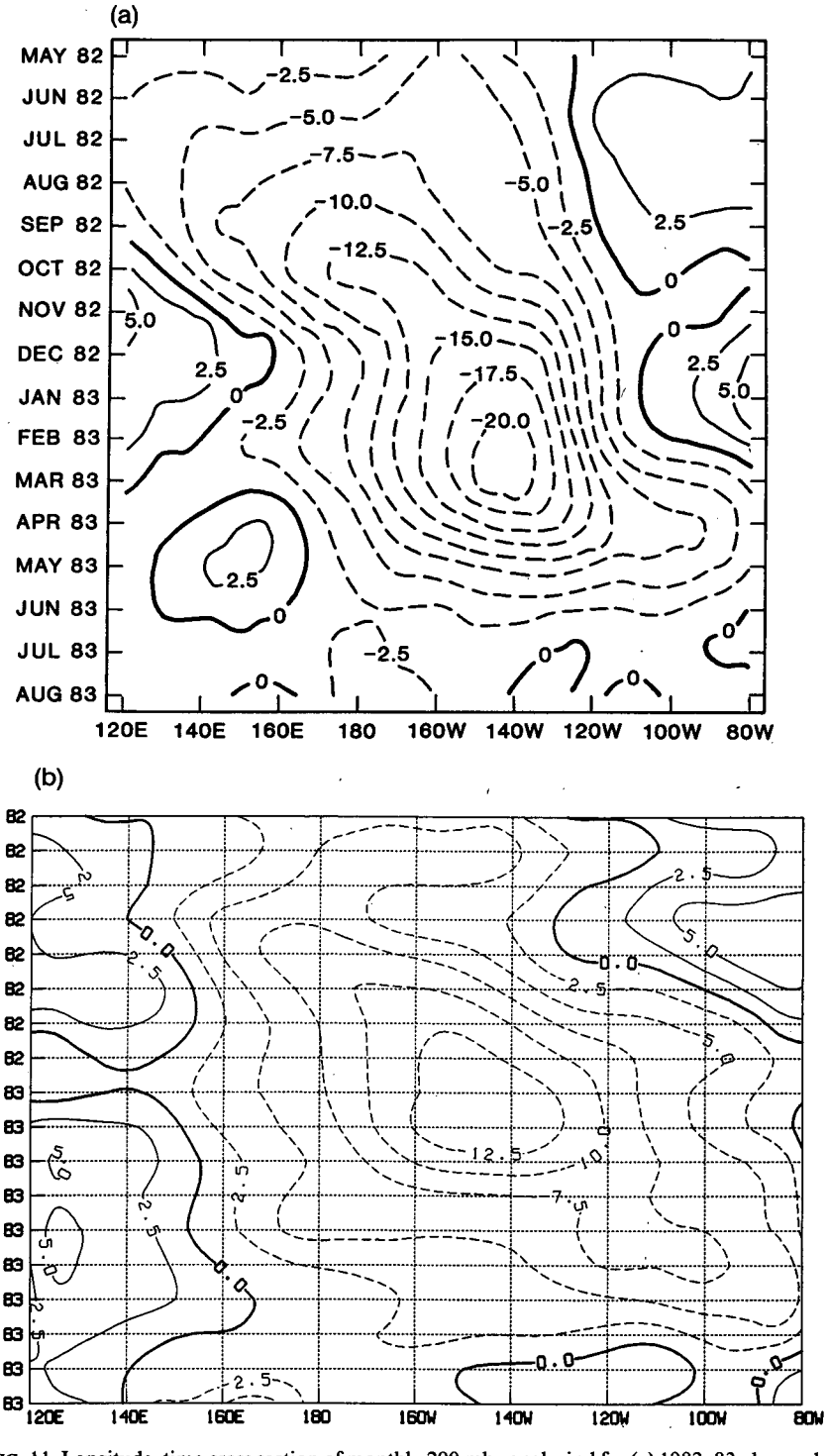

FIG. 11. Longitude–time cross section of monthly 200 mb zonal wind for (a) 1982–83 observed anomaly adopted from Arkin et al. (1983), and (b) simulated anomaly. Contour interval is 2.5 m s^{-1}. Dashed contours are negative.

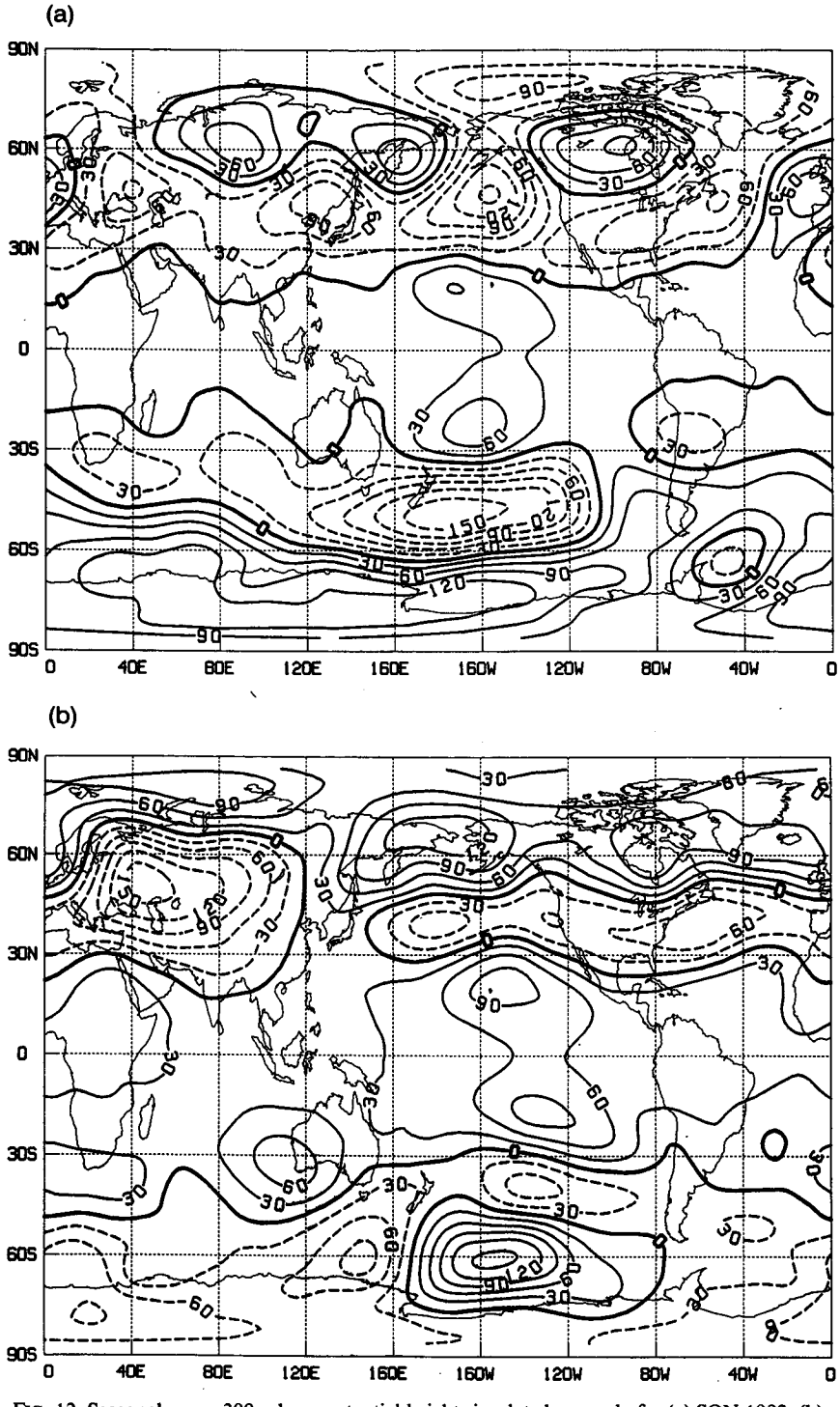

FIG. 12. Seasonal mean 300 mb geopotential height simulated anomaly for (a) SON 1982, (b) DJF 1982/83, and (c) MAM 1983. Contour interval is 30 m. Dashed contours are negative.

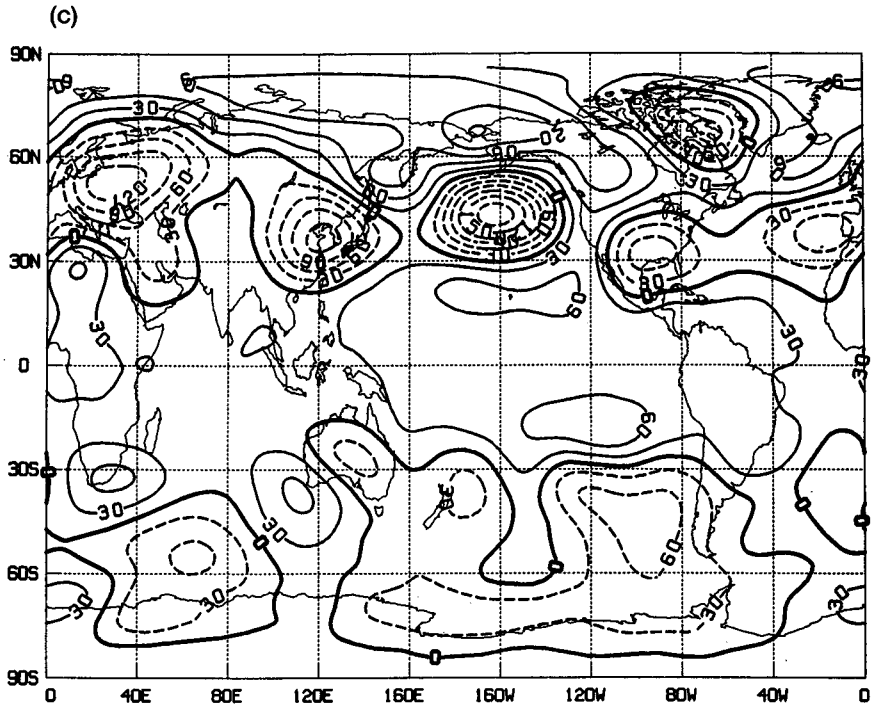

FIG. 12. (*Continued*)

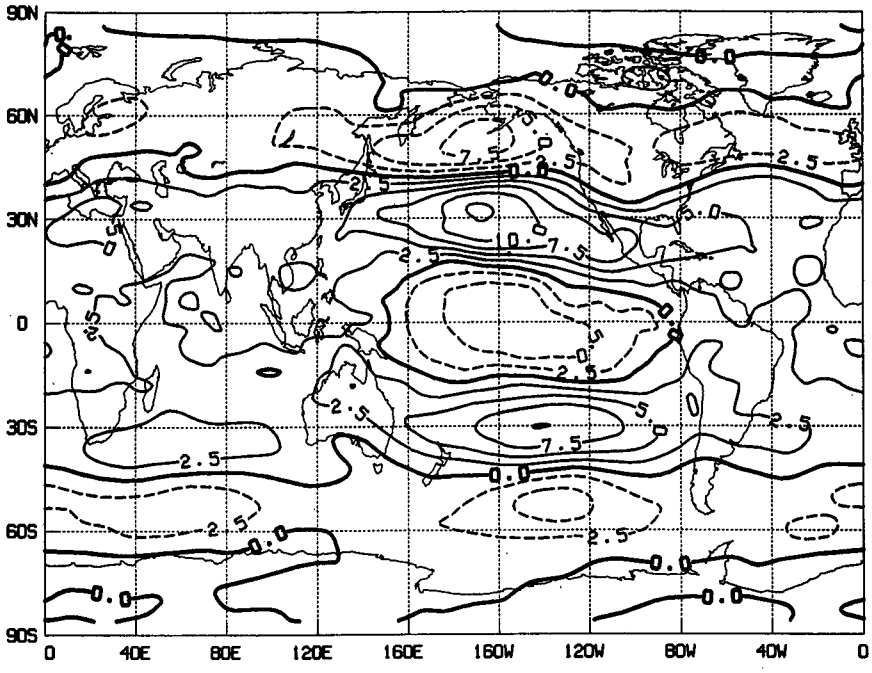

FIG. 13. May 1982–October 1983 18-month mean 200 mb zonal wind simulated anomaly. Contour interval is 2.5 m s^{-1}. Dashed contours are negative.

their statistical significance. This may be particularly important in the extratropics where the simulated variability is large.

Acknowledgments. The authors would like to thank L. Marx for his help with the model integrations and R. Reynolds of CAC for providing the sea surface temperature anomalies used in this study. We are grateful to Ms. L. Rumburg for drafting the figures and Mrs. Marlene Schlichtig and Ms. Marilyn Hopkins for their careful preparation of the manuscript. This research was supported by NASA's climate program through Grant NAGW-557, and jointly by the National Science Foundation and the National Oceanic and Atmospheric Administration under Grant ATM-8414660.

REFERENCES

Arkin, A., J. D. Kopman and R. W. Reynolds, 1983: *1982–1983 El Niño/Southern Oscillation Event Quick Look Atlas.* Climate Analysis Center, National Meteorological Center, NOAA/National Weather Service, Washington, DC, 20233.

Deardorff, J. W., 1972: Parameterization of the planetary boundary layer for use in general circulation models. *Mon. Wea. Rev.*, **100,** 93–106.

Fennessy, M. J., L. Marx and J. Shukla, 1985: General circulation model sensitivity to 1982–83 equatorial pacific sea surface temperature anomalies. *Mon. Wea. Rev.*, **113,** 858–864.

Geisler, J. E., M. L. Blackmon, G. T. Bates and S. Munoz, 1985: Sensitivity of January climate response to the magnitude and position of equatorial Pacific sea surface temperature anomalies. *J. Atmos. Sci.*, **42,** 1037–1049.

Lau, N. C., 1985: Modeling the seasonal dependence of the atmospheric response to observed El Niños in 1962–76. *Mon. Wea. Rev.*, **113,** 1970–1996.

Nihoul, J. C. J., 1985: *Coupled Ocean–Atmosphere Models.* Elsevier, pp. 767.

Palmer, T. N., and D. A. Mansfield, 1986a: A study of wintertime circulation anomalies during past El-Niño events using a high-resolution general circulation model. Part I: Influence of model climatology. *Quart. J. Roy. Meteor. Soc.*, **112,** 613–638.

——, and ——, 1986b: A study of wintertime circulation anomalies during past El Niño events using a high-resolution general circulation model. Part II: Variability of the seasonal mean response. *Quart. J. Roy. Meteor. Soc.*, **112,** 639–660.

Quiroz, R. S., 1983: The climate of the "El Niño" winter of 1982–83, a season of extraordinary climatic anomalies. *Mon. Wea. Rev.*, **111,** 1685–1706.

Randall, D. A., 1976: The interaction of the planetary layer with large-scale circulations. Ph.D. thesis, University of California, Los Angeles. pp. 247.

Rasmusson, E. M., and J. M. Wallace, 1983: Meteorological aspects of the El Niño/Southern Oscillation. *Science,* **222,** 1195–1202.

Shukla, J., 1984: Predictability of time averages: Part II. The influence of the boundary forcing. *Problems and Prospects in Long and Medium Range Weather Forecasting.* D. M. Burridge and E. Kallen, Eds., Springer Verlag, pp. 155–206.

——, and J. M. Wallace, 1983: Numerical simulation of the atmospheric response to equatorial Pacific sea surface temperature anomalies. *J. Atmos. Sci.*, **40,** 1613–1630.

——, and M. J. Fennessy, 1987: Prediction of time mean atmospheric circulation and rainfall: influence of Pacific SST anomaly. *J. Atmos. Sci.*, **44,** in press.

Tokioka, T., K. Yamazaki and M. Chiba, 1985: Atmospheric response to the sea surface temperature anomalies observed in early summer of 1983. *J. Meteor. Soc. Japan,* **63,** 565–588.

WMO, 1986: Workshop on comparison of simulations by numerical models of the sensitivity of the atmospheric circulation to sea surface temperature anomalies. WMO/TD—No. 138, WCP-121, World Meteorological Organization, Geneva, pp. 188.